

# The Effect of Metal Loading on Structural Characteristics and Low Temperature CO Oxidation Activity of Coprecipitated Co/Al<sub>2</sub>O<sub>3</sub>

Şeyma ÖZKARA<sup>1</sup>, Ayşe Nilgün AKIN<sup>2</sup>, Zülal MISIRLI<sup>1</sup>,  
Ahmet Erhan AKSOYLU<sup>1\*</sup>

<sup>1</sup>*Department of Chemical Engineering, Boğaziçi University,  
34342, Bebek, İstanbul-TURKEY*

<sup>2</sup>*Kocaeli University, Chemical Engineering Department, Veziroğlu Campus,  
41040, Kocaeli-TURKEY  
e-mail: aksoylu@boun.edu.tr*

Received 20.07.2004

The effect of metal loading on structural properties and CO oxidation activity of coprecipitated Co/Al<sub>2</sub>O<sub>3</sub> catalysts was investigated. The results indicated the participation of cobalt in the Co-Al skeleton for all coprecipitated samples. Environmental-SEM-EDXS studies showed that at loadings higher than ca. 15 wt.-%, cobalt formed layer-by-layer clusters on the surface; 16.8 wt.-% Co/Al<sub>2</sub>O<sub>3</sub> displayed the highest activity and stability in CO oxidation.

**Key Words:** Catalysis, Catalyst activation, Environment, Precipitation, CO oxidation, cobalt-alumina catalysts.

## Introduction

Carbon monoxide, a product of incomplete combustion or partial oxidation of carbonaceous materials, is the most wide spread gaseous hazard. Elimination of CO via catalytic CO oxidation is one way of reducing air pollution. Fuel processors, in which 3 catalytic reactions, indirect partial oxidation, water gas shift and preferential oxidation of CO, take place are used for producing pure H<sub>2</sub> to be fed to fuel cells. CO oxidation catalysts are also used in the preferential oxidation unit of the fuel processor for selective elimination of CO in order to obtain a pure H<sub>2</sub> stream <sup>1</sup>.

The catalytic oxidation of carbon monoxide on transition metal surfaces has attracted increasing attention <sup>2</sup>. In addition to precious metals, the first row transition metal oxides are known to be generally active as oxidation catalysts <sup>3</sup>. A series of papers have been published concerning low-temperature oxidation of carbon monoxide and hydrocarbons over various transition metal oxides. One of the examples of transition metal oxides used in this reaction is Co<sub>3</sub>O<sub>4</sub><sup>4-6</sup>. Cobalt oxide catalysts have been studied several times over

---

\*Corresponding author

the years, not only for their activity in CO oxidation but also for their use in CO hydrogenation<sup>6</sup>. Although it is known that the activity and product selectivity of Co-based catalysts depend not only on metal loading but also on the preparation method, almost all studies were performed on impregnated samples. On the other hand, our previous studies showed that coprecipitated Co/Al<sub>2</sub>O<sub>3</sub> has higher activity in CO hydrogenation than do impregnated catalysts<sup>7-9</sup>.

The effect of Co metal loading on physical properties and low-temperature CO oxidation activity of coprecipitated Co/Al<sub>2</sub>O<sub>3</sub> catalysts was investigated. The catalysts prepared were evaluated based on their total surface area (TSA), micro-scale structural and surface properties, and CO oxidation performances.

## Experimental

Co/Al<sub>2</sub>O<sub>3</sub> catalysts containing 2.4, 9.9, 13.3, 16.8 and 36 wt.-% Co were prepared by the coprecipitation of the hydroxides of cobalt and aluminum from the corresponding nitrates reacting in a basic solution. The detailed preparation procedure has been given elsewhere<sup>8,9</sup>.

Selected catalyst samples, which were calcined at 623 K for 2 h and then reduced at the same temperature under CO flow, were tested using environmental scanning electron microscopy (ESEM) to obtain information on their surface structure and metal dispersion. No coating was applied to the samples prior to the ESEM study. Their natural surface characteristics were studied using the appropriate microstructural characterization parameters in a field emission environmental scanning electron microscope (FE-ESEM, Philips XL30 ESEM FEG) equipped with an energy-dispersive X-ray spectrometry EDS (EDAX). The system has a maximum resolution of 2 nm. The experiments were performed at the Advanced Technologies Research and Development Center at Boğaziçi University.

TSA of Co/Al<sub>2</sub>O<sub>3</sub> catalysts calcined at 623 K for 2 h in a muffle furnace were measured on a Micromeritics Flowsorb II 2300 by N<sub>2</sub> adsorption from N<sub>2</sub>-He mixtures at liquid nitrogen temperature using a multi-point technique and the BET equation.

Reaction experiments for assessing catalytic performance were performed in a fixed-bed microreactor system connected online to a Shimadzu GC-8APT temperature programmable gas chromatograph equipped with a TCD. A molecular sieve 5A column was used in determination of the feed and product compositions. Samples ground to 45-60 mesh sizes were used in the reaction tests. The fresh samples were calcined at 623 K for 2 h in a muffle furnace and reduced at 623 K for 2 h with CO. All the reaction experiments were conducted isothermally at 373 K on freshly reduced samples with a CO/O<sub>2</sub> molar feed ratio of 1/21. The total gas flow rate was 50 mL/min. The catalyst sample weight was 0.5 g. All extra pure reactants (i.e. O<sub>2</sub> and CO), inert diluent (He), and reducing gas (CO) were fed from pressurized gas cylinders. The gas flow rates were controlled by Aalborg DFC digital mass flow controllers.

## Results and Discussion

Freshly reduced coprecipitated cobalt/alumina catalysts were tested using ESEM-EDXS to obtain information on their microstructural and metal dispersion properties. The different phases on the catalyst surface were discriminated using backscattered composition image mode (COMP-image). In all figures, the brighter parts are cobalt sites. EDX point analyses were performed for chemical composition of the phases. SEM images of 9.9, 16.8 and 36 wt.-% Co/Al<sub>2</sub>O<sub>3</sub> are given in Figures 1a-d.

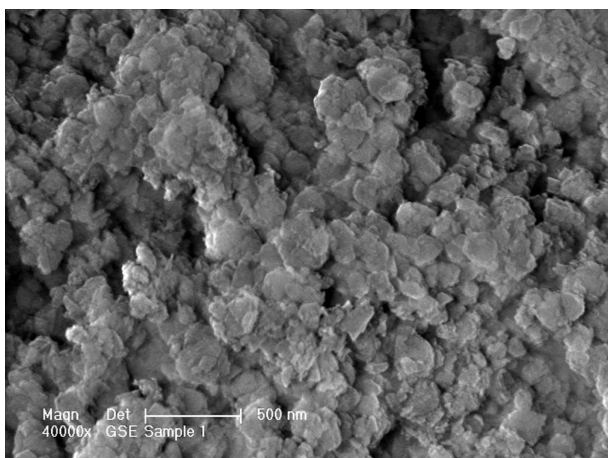


**Figure 1a.** ESEM image of 9.9 wt.-% Co/Al<sub>2</sub>O<sub>3</sub>. Composition image (X40,000). There is no Co agglomeration on the sample surface.

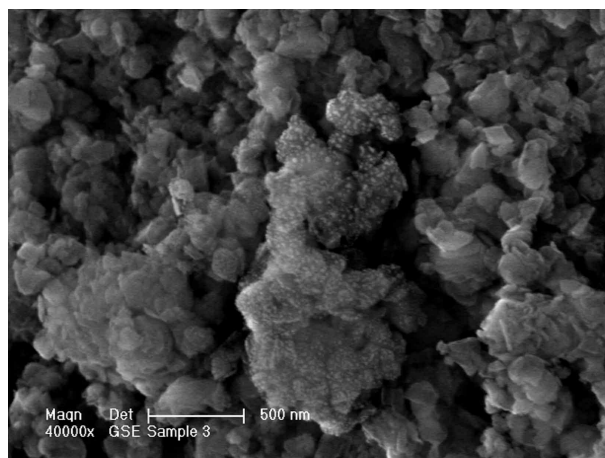


**Figure 1b.** ESEM image of 16.8 wt.-% Co/Al<sub>2</sub>O<sub>3</sub>. Composition image (X40,000). Co agglomerates start forming on the catalyst surface; these agglomerates will behave as the “nucleation centers” for cluster formation when Co loading is increased.

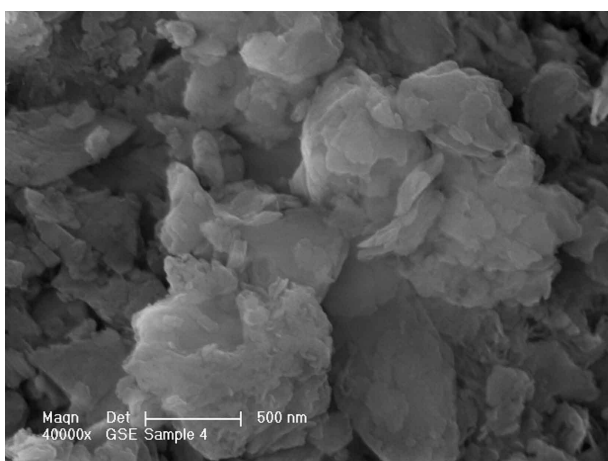


**Figure 1c.** ESEM image of 36 wt.-% Co/Al<sub>2</sub>O<sub>3</sub>. Composition image (X40,000). The detailed structure of the Co clusters formed. The image shows layer-by-layer structure of the Co clusters. Pores are formed between the Co layers.

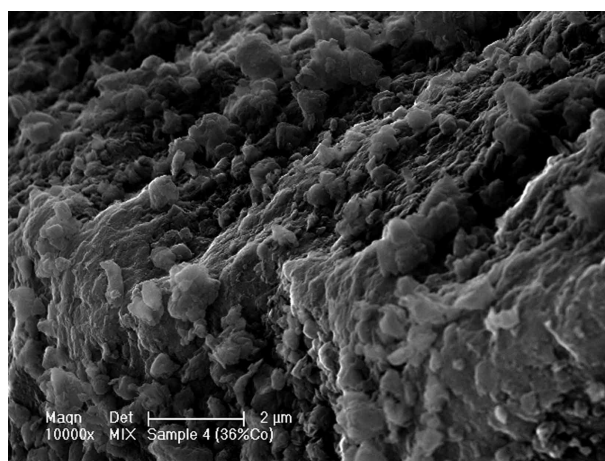


**Figure 1d.** ESEM image of 36 wt.-% Co/Al<sub>2</sub>O<sub>3</sub>. Composition image with tilted stage (X10,000). The image shows Co clusters at the catalyst surface and how they block the pores of the outer surface of the Co-Al skeletal structure.

At low cobalt loadings, it is observed that cobalt metal suspended on alumina integrates into the skeletal structure. Moreover, EDAX determined a very thin layer of Co on the surface, but no Co cluster formation (Figure 1a). At a cobalt loading of 16.8 wt.-%, the SEM figure shows that excess Co that cannot incorporate into the skeletal structure starts forming Co agglomerates, but these are still small nucleation centers and the Co amount on the outer surface is not enough for cluster formation (Figure 1b). At 36 wt.-%, on the other hand, the formation of layer-by-layer Co clusters is observed (Figures 1c, d). These clusters block the pores of the Co-Al skeletal structure, but, at the same time, form its own porous structure (Figure 1c). In Figure 1d, the microstructural details of how Co clusters blocked the pores of alumina surface is shown with the help of the tilted stage.

**Table 1.** Total surface areas of coprecipitated Co/Al<sub>2</sub>O<sub>3</sub> catalysts.

Co %	BET Area (m <sup>2</sup> /g)
2.4	176
9.9	265
13.3	290
16.8	243
36	214

BET surface areas of the samples were calculated from N<sub>2</sub> adsorption experiments in order to observe the effect of metal loading on physical properties of coprecipitated cobalt alumina catalysts. The results indicate that TSA passes through a maximum at 13.3 wt.-% Co loading. In coprecipitated catalysts, active metal plays a direct role in the formation of the physical structure, and thus the change in the metal loading may result in a formation of maximum in the surface area of the catalyst as a function of metal loading. This can be explained by 2 different roles of Co on the catalyst structure: (i) Co plays a direct role in the formation of skeletal structure of the catalyst; in this way, an increase in TSA up to ca. 15 wt.-% loading is possible with Co addition, and (ii) at higher loadings, on the other hand, excessive Co forms clusters on the catalyst surface that block the pores, but, at the same time, form its own porous structure. The TSA loss for highly loaded samples is rather limited since Co on the outer surface forms its own porous structure. This explanation is based on the comparative analysis of the data obtained from ESEM-EDXS discussed above. In a recent paper, a maximum in TSA with the variation in metal loading was also reported for coprecipitated Ni/Al<sub>2</sub>O<sub>3</sub>. It was proposed that above ca. 15 wt.%, nickel formed its own porous structure on the catalyst surface. Thus, the TSA values and SEM images in this study for Co/Al<sub>2</sub>O<sub>3</sub> also justify our explanations for the loss of surface area at high loadings for coprecipitated nickel<sup>10</sup>.

It should be noted that 2.4 wt.-% Co/Al<sub>2</sub>O<sub>3</sub> did not show any activity in CO oxidation under the reaction conditions used. During the preparation of low-loaded cobalt catalysts small cobalt oxide particles are formed. The thermal treatment under the reducing gas flow makes these small oxide particles react with the alumina support forming cobalt aluminate, which is not active in CO oxidation<sup>11</sup>. In our previous study<sup>7</sup>, XRPD patterns of reduced coprecipitated Co/Al<sub>2</sub>O<sub>3</sub> catalysts with less than 10% Co show the presence of a CoAl<sub>2</sub>O<sub>4</sub> phase, while Co<sub>3</sub>O<sub>4</sub>, Co and Al<sub>2</sub>O<sub>3</sub> are present in catalysts with 13.3% Co or above. Therefore, no catalytic activity for 2.4 wt.-% Co/Al<sub>2</sub>O<sub>3</sub> is likely to result from the formation of the fairly inactive spinel CoAl<sub>2</sub>O<sub>4</sub>, or encapsulation of cobalt by the Al<sub>2</sub>O<sub>3</sub> skeleton<sup>3,8,9</sup>.

Table 2 shows the CO oxidation activity of coprecipitated Co/Al<sub>2</sub>O<sub>3</sub> with various cobalt loadings during the first 2 h of the reaction at 373 K, which is a suitable temperature for both CO and O<sub>2</sub> chemisorption on cobalt oxide<sup>4</sup>, with an O<sub>2</sub>/CO molar feed ratio of 21/1 and a space-velocity of 10 mg mL/min. It is observed that all of the catalysts display ca. 100% CO conversion for the first hour of the reaction analysis. The high activity of the catalysts proves the beneficial effect of the coprecipitation method. Our SEM studies showed that coprecipitation permits the homogeneous distribution of cobalt in the alumina structure and permits the preparation of catalysts with extensive metal-support interaction, which allows the metal to have a direct influence on the catalyst structure. Between these samples, the highest stable activity was obtained on 16.8 wt.-% Co/Al<sub>2</sub>O<sub>3</sub>. The ESEM and BET results indicated that a 16.8 wt.-% Co load is just enough for the formation of small Co agglomerates on the outer surface of the catalysts. According to the results of our previous study<sup>7</sup>, 16.8 wt.-% Co/Al<sub>2</sub>O<sub>3</sub> catalysts have a 6.1

m<sup>2</sup>/g metal surface area, 6% dispersion and 18 nm crystallite size, while 13.3 wt.-% and 36 wt.-% Co/Al<sub>2</sub>O<sub>3</sub> catalysts have 4.7 and 6.6 m<sup>2</sup>/g metal surface areas, 7% and 3% dispersions, and 14 and 32 nm crystallite sizes, respectively. Comparing these results with the present study, the Co agglomerates on the outer surface of the 16.8 wt.-% Co/Al<sub>2</sub>O<sub>3</sub> catalyst are probably the most active sites having optimal size and dispersion for catalytic low-temperature CO oxidation. It should be noted that the conversions start to decrease after 30 min onstream for some of the samples, because when the surface chemistry, the distribution and ratio of sites for CO and oxygen adsorption are not optimal for stable CO oxidation performance, the active sites for oxygen adsorption may be covered by unused CO on the surface, leading to a scarcity of sites for oxygen adsorption. For these samples, the activity is suppressed by the strongly adsorbed CO on Co sites, which inhibits oxygen adsorption and leads to a decrease in activity levels over time.

**Table 2.** Effect of cobalt content on catalyst activity (O<sub>2</sub>/CO = 21/1, W/F = 10 mg mL/min, reaction temperature = 373 K).

Co %	CO Conversion (% mole)			
	30'	60'	90'	120'
9.9	100	100	95	90
13.3	100	88	84	81
16.8	100	100	100	100
36	100	100	98	95

## Conclusions

The results show that (i) it is possible to prepare catalysts with high metal content by the coprecipitation method with a limited loss of surface area, (ii) the layer-by-layer formation of Co clusters on the Co-Al skeleton and the arrangement of their own porous structural pattern act like a promoter for the enhanced conversion of carbon monoxide, and (iii) 16.8 wt.-% Co/Al<sub>2</sub>O<sub>3</sub> displays the best catalytic performance as it does not lose stability and stays at 100% CO conversion during the reaction.

## Acknowledgment

This study was supported by Boğaziçi University through the projects DPT 01K120300 (DPT: State Planning Organization of Turkey), BAP 00HA501, and BAP 01S106.

## References

1. Ş. Özkara and A.E. Aksoylu, **Appl. Catal. A** **251**, 75-83 (2003).
2. G. Gürdağ and T. Hahn, **Appl. Catal. A** **192**, 51-55 (2000).
3. M. Skoglundh, A. Törnqvist, E. Fridell, E. Jobson and P. Thormählen, **Appl. Catal. B** **14**, 131-145 (1997).
4. F. Grillo, M.M. Natile and A. Glisenti, **Appl. Catal. B** **48**, 267-274 (2004).
5. Y.J. Mergler, J. Hoebink and B.E. Nieuwenhuys, B. E., **J. Catal.** **167**, 305-313 (1997).
6. P. Thormählen, M. Skoglundh, E. Fridell and B. Andersson, **J. Catal.** **188**, 300-310 (1999).

7. A.N. Akın, A.E. Aksoylu and Z.İ. Önsan, **React. Kinet. Catal. Lett.** **66**, 393-399 (1999).
8. A.N. Akın and Z.İ. Önsan, **J. Chem. Technol. Biotechnol.** **69**, 337-344 (1997).
9. A.N. Akın and Z.İ. Önsan, **J. Chem. Technol. Biotechnol.** **70**, 304-310 (1997).
10. A.E. Aksoylu, A.N. Akın, Z.İ. Önsan and D.L. Trimm, **Appl. Catal. A** **145**, 185-193 (1996).
11. J. van de Loosdrecht, M. van der Haar, A. M. van der Kraan, A. J. van Dillen and J.W. Geus, **Appl. Catal. A** **150**, 365-376 (1997).